Spring 2017

# Mutagenic and Spectroscopic Investigation of pH Dependent CooA DNA Binding

Brian R. Weaver
*Valparaiso University*

# Mutagenic and Spectroscopic Investigation of pH Dependent CooA DNA Binding

by

Brian R. Weaver

Honors Work in Chemistry
For Chemistry-498
Advised by Dr. Robert W. Clark

College of Arts and Sciences
Valparaiso University

Spring 2017

# Mutagenic and Spectroscopic Investigation of pH Dependent CooA DNA Binding

By: Brian R. Weaver

**Abstract:**

The carbon monoxide (CO) sensing heme protein, CooA, is a transcription factor which exists in several bacteria that utilize CO as an energy source. CooA positively regulates the expression of *coo* genes in the presence of CO such that the corresponding proteins may metabolize CO. The present studies have yielded the unexpected result that Fe(III) CooA binds DNA tightly at pH < 7, deviating from all previously reported work which indicate that CooA DNA binding is initiated only when the exogenous CO effector reacts with the Fe(II) CooA heme. This observation suggests that the disruption of one or more salt bridges upon effector binding may be a critical feature of the normal CooA activation mechanism. To test this possibility, several protein variants that eliminated a selected salt bridge for the CooA homolog from *Rhodospirillum rubrum* were prepared via site-directed mutagenesis. Samples of these variant proteins, which were overexpressed in *Escherichia coli*, were then characterized by spectroscopic methods and functional assays to investigate the impact these mutations had on CooA heme coordination structure and DNA-binding activity. Results of this work are presented in light of the accepted CooA activation mechanism.

**Introduction:**

Carbon monoxide (CO) oxidation activator, CooA, is a bacterial heme protein that senses the presence of CO *in vivo* (Figure 1). In the presence of CO, CooA, which is composed of two equivalent polypeptide chains (i.e. two monomers), changes conformation and gains the ability to bind a specific DNA promoter sequence ($P_{coof}$) upstream of what is termed the *coo* operon of genes. These *coo* genes encode for proteins that ultimately oxidize CO to carbon dioxide thus enabling the organism to grow using CO as a sole energy source.[1] CooA is a member of the CRP/FNR family, a set of related proteins which exhibit DNA binding activity that is allosterically regulated by small molecules. CooA homologs have been discovered in both facultative and obligate anaerobes This work reports results for studies performed for the CooA homolog from the facultative anaerobe *Rhodospirillum rubrum* (*Rr*) and the obligate anaerobe *Carboxydothermus hydrogenoformans* (*Ch*), which is a thermophile.

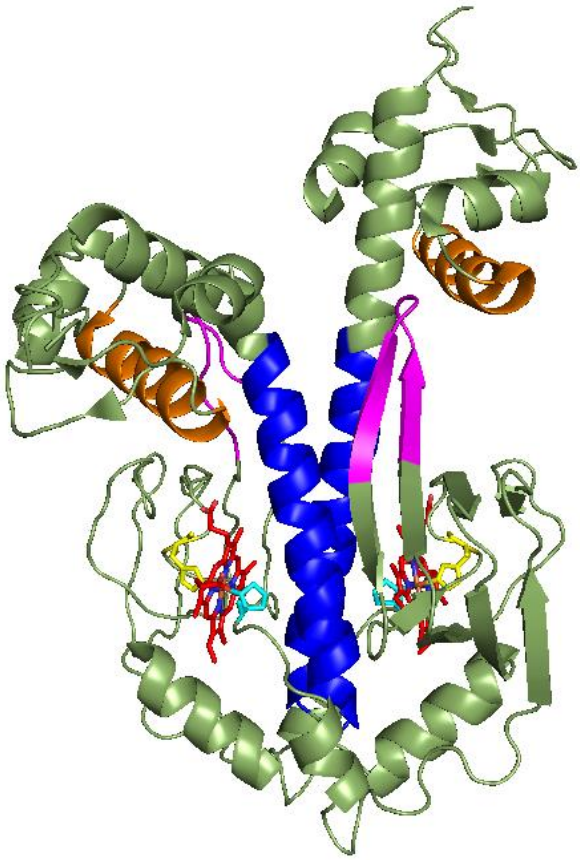

**Figure 1.** Inactive structure of CooA derived from *Rhodospirillum rubrum* (PDB 1FT9).[2] The b-type hemes are shown in red. The N-terminal heme ligands are shown in cyan. The distal heme ligands are shown in yellow. The conserved β4/5 loops are shown in purple. The central C helices are shown in blue. The F helices that bind the major groove of DNA upon conformational change are shown in orange.

*In vivo*, CO binds to the heme iron within CooA. This binding event triggers conformational change allowing CooA to bind DNA. Studies on the process by which CooA undergoes conformational change draws upon insight from advanced spectroscopy and x-ray crystallography structures and are due directly to changes in the coordination states of the CooA heme groups. Previous research indicates that the CooA heme exists in three physiologically-relevant coordination states that affect the protein's structure and function. These states are termed Fe(III), and Fe(II) and Fe(II)-CO and are shown in Figure 2.

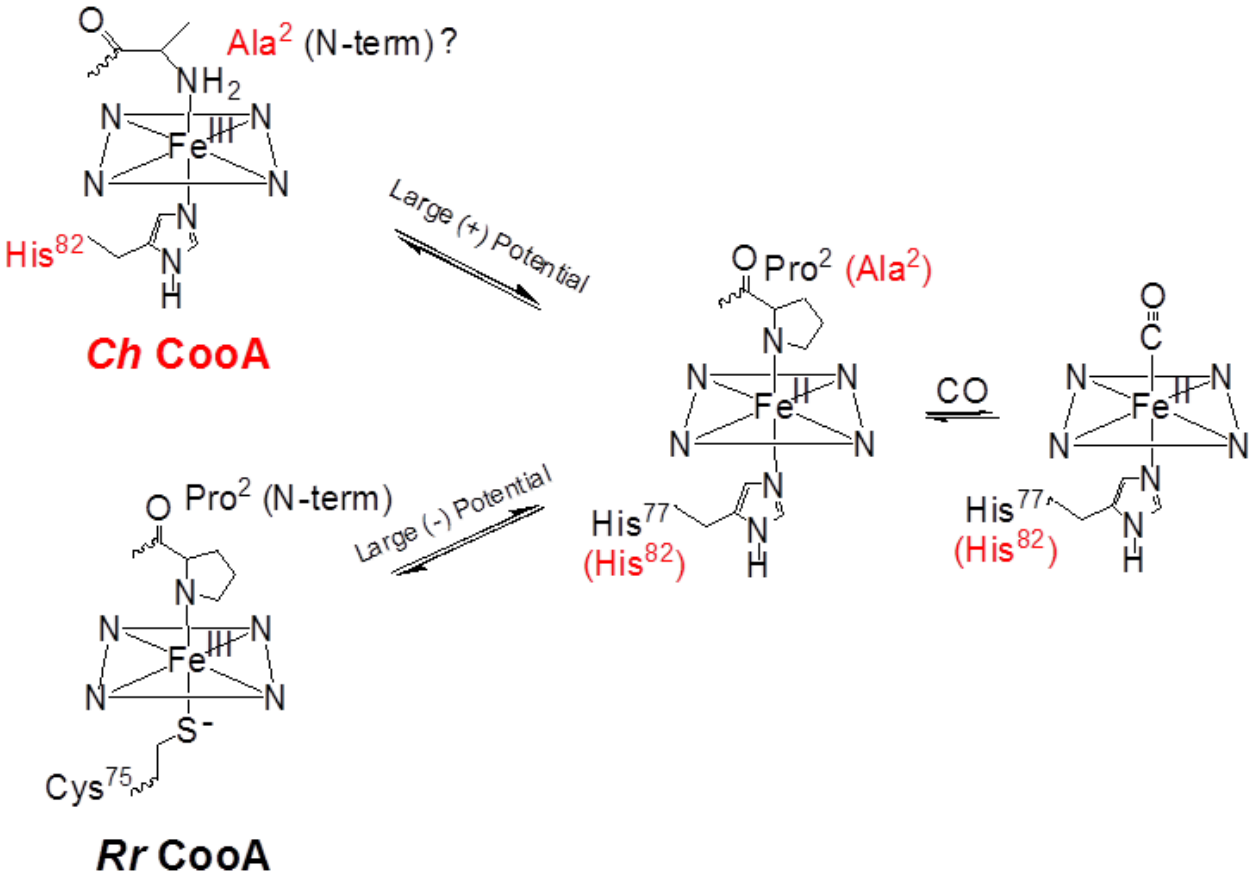


**Figure 2. S**chematic describing the ligand structure of *Ch.* and *Rr.* CooA in the Fe(III) (left), Fe(II) (middle), and Fe(II)-CO forms. The final Fe(II)-CO ligand structure corresponds to CooA in the active conformation.

All structures shown in Figure 2 are 6-coordinate heme structures, meaning that the iron is forming coordinate bonds with 6 distinct ligands: four from the nitrogen atoms within the heme ring and two axial bonds to protein ligands or CO. A 5-coordinate heme structure refers to structures in which one of the axial ligands (typically $Pro^2$, $Ala^2$ or CO) is removed, leaving 5 coordinate bonds to the central iron.

CooA activation begins with the reduction of the Fe(III) center to Fe(II). Additionally, *Rr* CooA couples this single electron reduction with a distal ligand exchange from $Cys^{75}$ thiolate to a $His^{77}$ (Figure 2). In all other characterized CooA homologs, including *Ch* CooA, a histidine remains the ligand in both the ferric and ferrous heme states; however, despite these differences,

in all cases neither the Fe(III) or Fe(II) states of CooA are capable of binding DNA at physiological pH, i.e. pH 7.4.[3] Finally, CO, upon interaction with CooA, binds to the Fe(II) heme and displaces the N-terminal proline, which serves as the distal heme ligand and is part of a long "tail structure" from the other monomer.[4] Studies have suggested that the N-terminal tail structure migrates toward the DNA binding domain, making contacts with both the DNA and CO binding domains.[5] However, deletion mutants that shorten the tail are not sufficient to provide CO-independent activity.[4]

In addition to displacement of the N-terminal residue, resonance raman data have suggested that the heme moves into an adjacent hydrophobic cavity formed on the C helix upon CO binding.[6] This translation strains the Fe-His[77] bond and triggers rearrangement of the C helix. A crystal structure of active CooA (Figure 3), achieved by mutations of two amino acids in the CooA C helix to leucine, reinforces the necessity of C helix rearrangement.[7] Furthermore, the active CooA crystal structure and a crystal structure of a related transcription factor, cAMP receptor protein (CRP) shown in Figure 4, both suggest the DNA binding domain of CooA must rearrange to facilitate DNA binding.[7] The CooA F helices must migrate from the bottom of the DNA binding domain to the top to facilitate insertion into the major groove of the DNA recognition sequence (Figure 4).

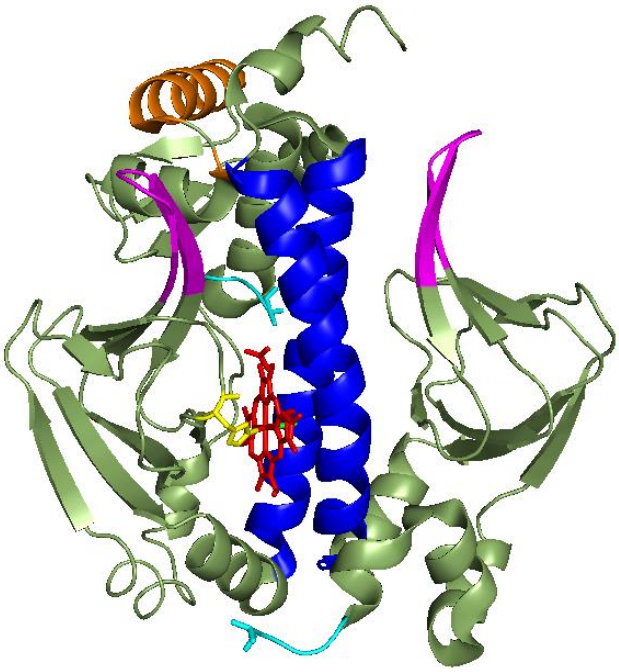

**Figure 3.** Active structure of CooA derived from *Carboxydothermus hydrogenoformans* (PDB 2HKX).[7] The hemes are shown in red. The N-terminal heme ligands are shown in cyan. The distal heme ligands are shown in yellow. The proximal heme ligand, CO, is shown in green. The conserved β4/5 loops are shown in purple. The central C helices are shown in blue. The F helices that bind the major groove of DNA are shown in orange.

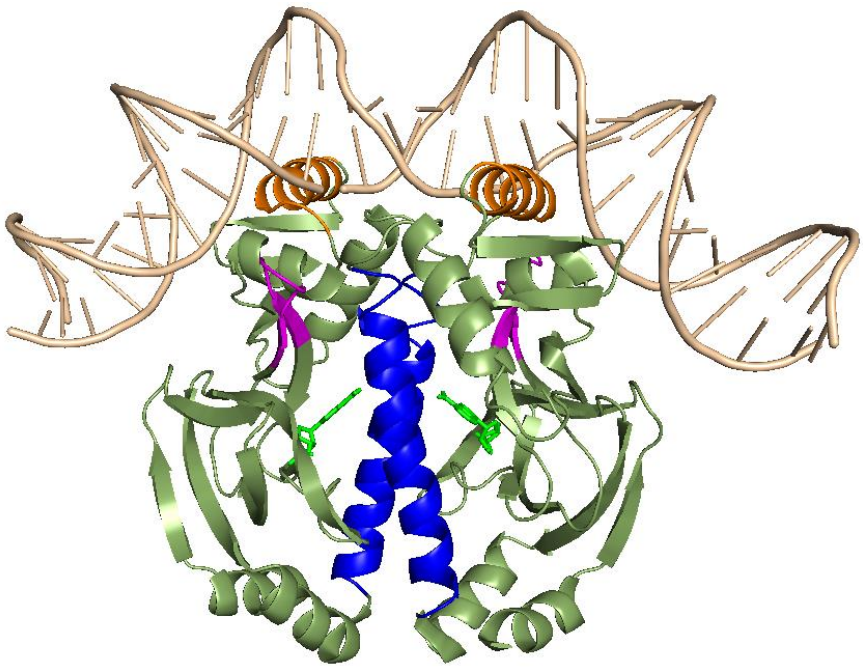

**Figure 4.** Active structure of cAMP Receptor Protein derived from Escherichia coli (PDB 1CGP).[8] The allosteric effector, cAMP, is shown in green. The distal heme ligands are shown in yellow. The conserved β4/5 loops are shown in purple. The central C helices are shown in blue. The F helices that bind the major groove of DNA are shown in orange.

Since CooA-DNA binding is a well understood event, laboratory methods have utilized this phenomenon to quantify CooA activity *in vitro* via a fluorescence anisotropy assay.[9] Fluorescence anisotropy describes a phenomenon in which a fluorophore excited with plane polarized light will emit fluorescence with unequal intensities with respect to polarization planes. Anisotropy is quantified using Equation 1,

$$A = \frac{I_{\parallel} - I_{\perp}}{I_{\parallel} + 2I_{\perp}} \quad [1]$$

where A represents fluorescence anisotropy, $I_{\parallel}$ represents fluorescence parallel to incident radiation and $I_{\perp}$ represents fluorescence perpendicular to incident radiation. The functional assay includes DNA oligomers representing the CooA recognition sequence that are tagged with a fluorophore. Free fluorescent DNA molecules undergo relatively fast tumbling rates in solution. This leads to low fluorescence anisotropy when the sample is exposed to polarized light. Upon a CooA binding event, an increase in anisotropy occurs due to a decrease in the tumbling rate of the fluorophore because of a drastic increase in size of the CooA:DNA bound complex. This effect is encapsulated in Equation 2,

$$A = \frac{A_0}{1 + \left(\frac{\tau}{\varphi}\right)} \quad [2]$$

where $A_0$ represents the lower limit of anisotropy, τ represents fluorescence lifetime (the length of time the fluorophore spends in the excited state prior to fluorescence), and ϕ represents the

rotational correlation time (the time it takes the molecule to rotate one radian).[9] Therefore, as the rotation of a molecule increases, anisotropy will approach the lower limit.

Lundblad, et al. have derived an equation which describes increasing fluorescence anisotropy as a function of increasing DNA-binding protein concentration. This equation is based upon a dynamic equilibrium in which a DNA-binding protein, P, is interacting with a sequence of fluorescently-tagged DNA, L, resulting in the associated complex, P:L (Equation 3).

$$P + L \rightarrow P{:}L \qquad [3]$$

This system has an associated equilibrium constant $K_a$ expressed in terms of the concentrations of P, L and P:L, respectively (equation 4).

$$K_a = K_d^{-1} = \frac{[P{:}L]}{[P][L]} \qquad [4]$$

This equation also notes the relationship between $K_a$ and $K_d$, which is the standard quantity for reporting DNA binding affinity of proteins. From this expression, Lundblad et al arrive at equation 5,

$$A = A_f + \left(A_b - A_f\right) * \frac{\left(1+K_a[P]+K_a[L]-\sqrt{(1+K_a[P]+K_a[L])^2-4[P][L]K_a^2}\right)}{2[L]K_a} \qquad [5]$$

where $A_f$ represents the anisotropy of unbound DNA and $A_b$ represents the anisotropy of the protein:DNA complex.[10] Since [L] is a constant determined by method and [P] is varied by each sample, experimental fluorescence anisotropy data may be fit to this equation by non-linear least squares analysis to provide an experimental $K_d$ value.

Electronic absorption spectroscopy has also been a useful method of investigating the coordination structure of the heme iron. Wild type *Rr* CooA in the Fe(III) state exhibits a Soret

peak at 424 nm corresponding to a 6-coordinate, low-spin heme. Upon reduction of this species to the Fe(II) state, a significant increase in the extinction coefficient of the Soret peak at 424 nm is observed.[4] Upon formation of the Fe(II)-CO state, the Soret peak shifts to 422 nm. Previous research has also characterized a second Soret peak at 385 nm when the N-terminal $Pro^2$ ligand is displaced by mutagenic or chemical methods; this is termed a 5-coordinate, high-spin heme.[4] Previous experiments by Clark et al. have observed that the N-terminus shortening CooA variant, ΔP3R4, exhibits significant absorbance at 385 nm at pH 7 and approximately 100% high-spin, 5-coordinate heme at pH 3.[4]

In this study, the first instance of CooA DNA binding in the Fe(III) state is reported. This activity is observed in acidic conditions because of serendipitous discovery derived from anisotropy assays in which ascorbic acid is used as reducing agent in place of sodium dithionite. pH-induced activity of *Rr* wild-type CooA is fully characterized from pH 3-8. Additionally, assays which study the reversibility of DNA binding activity are also reported. pH-induced activity is hypothesized to arise due to protonation of the N-terminal heme ligand and loss of a salt bridge which stabilizes the inactive conformation. To test this hypothesis, conserved salt bridges were identified, and CooA variants which removed the electrostatic interaction were produced and subsequently characterized using electronic absorption spectroscopy and a fluorescence anisotropy assay.

**Materials & Methods:**

*Site Directed Mutagenesis:*

Template plasmid DNA was isolated using QIAprep Spin Miniprep Kit (Qiagen) from *E. coli* strains UQ3454, which contain the wild-type *Rr* CooA gene plus seven histidine residues,

and UQ3566, which contains an identical CooA gene except that residues P3 and R4 have been deleted.[9] Plasmid isolation was completed using the centrifugation protocol provided by Qiagen and an AArdvark™ Personal Microcentrifuge (Southwest Science). The concentrations of these isolated plasmids were determined by electronic absorption spectroscopy using a CLARIOstar® microplate reader (BMG Labtech). Desalted DNA oligomers were purchased from Integrated DNA Technologies for use as primers. Primer sequences are shown in Table 1.

**Table 1.** Site Directed Mutagenesis Primer Sequences

| Primer Name | Sequence |
|---|---|
| *Rr* D72A FW | 5'-CCTGACCTCGGGCGCCATGTTTTGCATGC-3' |
| *Rr* D72A RV | 5'-GCATGCAAAACATGGCGCCCGAGGTCAGG-3' |
| *Rr* R118D FW | 5'-ATCGCCATCCTCGGCGATGCGCTGACCTCGTGC-3' |
| *Rr* R118D RV | 5'-GCACGAGGTCAGCGCATCGCCGAGAATGGCGAT-3' |
| *Rr* A114K R118D FW | 5′-GCCTGGGGGCTGATCAAAATCCTCGGCGATGCGCTGACCTCGTGC-3′ |
| *Rr* A114K R118D FW | 5′-GCACGAGGTCAGCGCATCGCCGAGGATTTTGATCAGCCCCCAGGC-3′ |

Site directed mutagenesis was completed using GeneArt® Site-Directed Mutagenesis System (Invitrogen) and AccuPrime™ Pfx DNA Polymerase (Thermo-Fisher Scientific). Polymerase chain reaction (PCR) reactions were assembled into PCR tubes as outlined in Table 2.

**Table 2.** PCR Reaction Mix Contents.
* included in GeneArt® Site-Directed Mutagenesis System

| **Solution** | **Amount (µl)** |
|---|---|
| *pfx* Reaction Mix | 5 |
| 10x Enhancer* | 5 |
| Primer Solution (10µM) | 1.5 |
| Template DNA (20 ng/µl) | 1 |
| DNA Methylase (4U/µl)* | 1 |
| 2.5x S-adenosyl methionine* | 2 |
| *pfx* DNA polymerase | 0.4 |
| PCR water* | 32.6 |

PCR tubes were mixed by pipetting and placed in Mastercycler® ep 5341 (Eppendorf) and reactions were ran using the parameters shown in Table 3.

**Table 3.** PCR Reaction Thermocycling Parameters

| Cycle Number | Temperature (°C) | Time | Repetitions |
|---|---|---|---|
| 1 | 37 | 15 min | 1 |
| 2 | 94 | 2 min | 1 |
| 3 | 94 | 20 s | 15 |
| | 57 | 30 s | |
| | 68 | 2 min | |
| 5 | 68 | 5 min | 1 |
| 6 | 4 | Hold | 1 |

After thermocycling was completed, the recombination reaction was assembled as shown in Table 4. Note that all reaction contents were provided in GeneArt® Site-Directed Mutagenesis System.

**Table 4.** Recombination Reaction Contents.

| **Solution** | **Amount (µl)** |
|---|---|
| 5x reaction buffer | 4 |
| PCR product | 4 |
| 10x enzymer mix | 2 |
| PCR water | 10 |

The recombination reaction was incubated at room temperature. After 10 minutes, 1µl of 0.5M EDTA was added to the mix to quench the reaction.

One Shot® MAX Efficiency® DH5α™-T1R competent cells (Invitrogen) were thawed on ice for 5 minutes. A total of 2 µl of recombination product was added to these cells. The mixture was then gently mixed by rocking and the cells were incubated surrounded in ice for 12 minutes. Afterward, the cells were heat shocked at 42°C for 30 seconds followed by a second incubation covered in ice for 2 minutes. A total of 2 µl of 40°C SOC medium (Invitrogen) was added to the cell solution using sterile technique. A total of 250 µl of this mixture was then plated onto an LB plate containing 100 µg/ml ampicillin and 1.5% agar. These plates were incubated overnight at 37°C. Single colonies were picked and streaked on fresh 1.5% agar LB + amp plates for further use.

Plasmid from transformed DH5α *E. coli* strains was isolated using the method described above. These mutated plasmids were transformed into the *E. coli* strain VSJ6737 provided by Valley Stewart, as this cell strain provides greatly enhanced CooA expression.[11] Resulting colonies were streaked onto fresh 1.5% agar LB + amp plates and submitted for DNA sequencing at the University of Chicago Comprehensive Cancer Center DNA Sequencing Facility. Sequencing was completed using the 1233 rev primer to confirm mutations were incorporated properly.

*Buffer and Media Preparation:*

In general, all buffers were prepared using the following protocol. Solid buffer (Table 5) and solid sodium chloride were dissolved in 100 ml of Milli-Q® purified water to bring their concentrations to 50 mM and 100 mM, respectively. Prior to diluting to final volume, pH was set to the appropriate concentration using 3 M hydrochloric acid or 3 M sodium hydroxide and a pH electrode (Extech) and a MicroLab interface FS-524. The pH meter was calibrated using pH4, 7 and 10 Hydrion® buffer solution capsules (Micro Essential Lab).

**Table 5.** Buffering reagents used in corresponding pH buffers.

| pH of Buffer | Buffering Component Used |
|---|---|
| 3 | sodium phosphate (dibasic, Sigma) |
| 4 | sodium acetate (Sigma) |
| 5 | sodium acetate (Sigma) |
| 6 | 2-(N-Morpholino)ethanesulfonic acid (MES) (sodium salt, Sigma) |
| 7 | 3-(N-Morpholino)propanesulfonic acid (MOPS) (sodium salt, Sigma) and sodium phosphate (dibasic, Sigma) |
| 8 | N-[Tris(hydroxymethyl)methyl]-3-aminopropanesulfonic acid (TAPS) (sodium salt, Sigma) |
| 12 | sodium phosphate (dibasic, Sigma) |

The 2x LC media was prepared by dissolving 20 g typtone, 10 g NaCl, 10 g yeast extract [all from Thermo-Fisher Scientific] into approximately 900 mL of Milli-Q® purified water. A

total of 10 mL of ferric citrate solution (0.28g/l hydrogen borate, 1.0g EDTA (disodium salt, dihydrate, Sigma, pH 7.0) is added and pH set to 7.5 as described above. The solution was then diluted to 1 L and autoclaved.

*CooA overexpression in E. coli:*

Preparation of *E. coli* strains used for CooA expression has been previously described.[15] Strains included UQ3454 (*Rr* Wt), UQ3566 (*Rr* ΔP3R4) and UQ3782 (*Ch* Wt) These cells were streaked on LB plates containing 100 mg/L ampicillin and 1.5% agar and incubated at 37°C for approximately 20 hours. An individual colony from these plates was placed in an Erlenmeyer flask filled with 50 mL of 2xLC media with 100 mg/L ampicillin. This reaction mixture was placed in a shaker incubator for 14-16 hours at 220 rpm and 37°C. After incubation, 5 mL of liquid culture was transferred to a 1L Erlenmeyer flask filled 500 mL of 2xLC media with 100 mg/L ampicillin. The resulting culture was incubated at 32°C and 220 rpm until the culture reached an optical density of 0.5(±0.05) at 600 nm, at which point Isopropyl β-D-1-thiogalactopyranoside (IPTG) was sterile filtered into solution to a final concentration of 500 mM. This culture was allowed to grow for 14-16 hours under the same conditions. Finally, the cells were harvested from the liquid culture by centrifuge at 4,000 rpm for 1 hour using a Jouan CR412 centrifuge.

*CooA purification with His tag:*

Cells were resuspended in 4.5 mL of MOPS buffer (25mM MOPS, 100mM NaCl, pH 7.5) per gram of cell mass. The pellet was homogenized using a dounce tissue homogenizer (15ml, pyrex). Solid lysozyme (dialyzed, lyophilized powder, Sigma-Aldrich) was added to provide a 10% w/v concentration. The reaction mixture was stirred for 1 hour at room

temperature. The mixture was then placed in a -5°C salt water bath and sonicated for 20 minutes, pulsing every other second at 35% amplitude (Vibracell VCX750, Sonics). The mixture was then centrifuged at 20,600xg and 4°C for one hour (Allegra 64R High Speed Centrifuge, F0850 rotor, Beckman-Coulter). The supernatant was moved to a separate container. To the supernatant, ammonium sulfate solution was added one drop per second to a final concentration of 40 %. The solution was then centrifuged at 20,600 xg and 4°C for 1 hour. The supernatant was decanted and the precipitate was resuspended in 2-5 mL of buffer A (25mM phosphate, 500mM NaCl, 20mM imidazole (Alfa Aesar), pH 7.5). Two 1ml HisTrap FF columns (GE Healthcare) attached in tandem were equilibrated with 20ml of buffer A and the protein was loaded onto the column using an ÄKTA Prime Plus column purification system (GE Healthcare). The column was further washed with 20 ml of buffer A and the protein was eluted from the column by running a step gradient from buffer A to buffer B (Buffer A with 200mM imidazole) over 40 mL while collecting 2 mL fractions. Resulting red fractions were analyzed via UV-Visible spectroscopy for the protein and heme Soret bands. The five fractions with the highest ratio of iron to protein (determined by electronic absorption spectroscopy) were combined, concentrated via 40% ammonium sulfate precipitation and centrifugation. Resuspension was achieved with buffer B and the final solution run through a desalting column. Heme concentration was calculated via electron absorption spectroscopy and reported Soret extinction coefficients (*Rr* Wt $\varepsilon_{424}$ = 104$mM^{-1}cm^{-1}$; ΔP3R4 $\varepsilon_{387}$ = 83.2$mM^{-1}cm^{-1}$; and *Ch* Wt $\varepsilon_{414}$ = 121$mM^{-1}cm^{-1}$).[12,13]

CooA variants, D72A and ΔP3R4, were purified using a modified procedure. After cell-free lysate was procured, the solutions were transferred to a fresh centrifuge tube and spun for an extra hour at 20,600 xg and 4°C. A total of 50 mL of supernatant was then applied directly to the

$Ni^{2+}$ column using the ÄKTA Prime Plus, washed with 50ml of buffer A and eluted as described above. From here, the purification of these variants was identical to that of wild-type proteins.

*DNA Binding Anisotropy Assay:*

Fourteen CooA samples ranging from 50 μM - 20 nM were prepared via serial dilution. Using these CooA samples, final anisotropy samples were prepared in 6 mm x 50 mm culture tubes (Fisherbrand) containing 8 nM – 2000 nM CooA, 8mM $CaCl_2$, 75mM pH buffer and 6.4nM of a DNA 24-mer dimer representing the $P_{coof}$ promoter sequence. The 26-mer, 5'-ATAACTGTCATCTGGCCGACAGACGG-3', was covalently labeled with the fluorophore Texas Red at the 5' end (Integrated DNA Technologies). Each sample was analyzed via a PC-1 fluorometer (ISS) for fluorescence anisotropy. Samples were exposed to 585nm light utilizing polarized filters for excitation and emitted light. Slits were 2 mm for incident radiation and 1mm slit for the sample. For all measurements, measured uncertainty was determined to be approximately 0.001. Reversibility experiments were completed by preparing and analyzing samples as using the standard protocol followed by a second analysis after pipetting 2μl of concentrated hydrochloric acid or sodium hydroxide. Solution pH values were confirmed using Hydrion® pH indicator test strips (Micro Essential Lab). Anisotropy vs CooA concentration curves were fitted to Equation 5 via non-linear least squares analysis using SigmaPlot software.

*Electronic Absorption Spectroscopy:*

Electronic absorption spectra were recorded at room temperature using an Agilent 8453 UV-Vis spectrophotometer (Agilent Technologies). Heme spectra were recorded using quartz, semi-micro cuvettes.

**Results and Discussion:**

Fluorescence anisotropy assays of *Rr* wild-type CooA at pH 3, 5, 6, 7, 8 and 12 are shown in Figure 5.

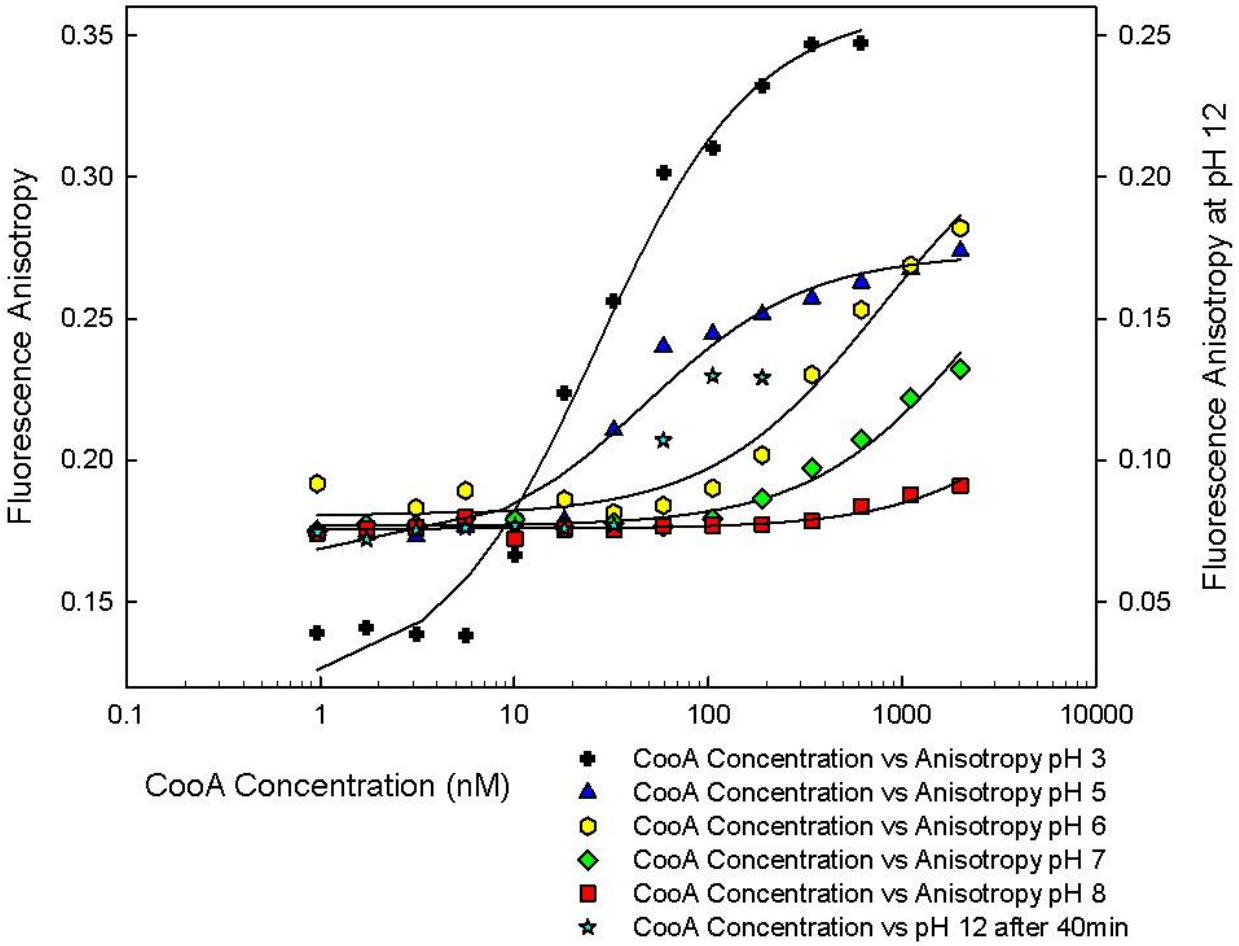


**Figure 5.** Fluorescence anisotropy plotted versus CooA concentration for samples containing *Rr* (pH 3-8) or *Ch* CooA (pH 12 after 40 min), calcium chloride, Texas Red-tagged DNA and various buffers. This graph demonstrates a decrease in $K_d$ value as pH decreases, suggesting that CooA somehow attains its active conformation and is binding to DNA.

The data reported in Figure 5 demonstrates the capability of wild-type CooA to bind DNA at pH ≤5. Nonlinear curve fits to Equation 3 provided the $K_d$ values reported in Table 6.

**Table 6.** CooA:DNA $K_d$ values of *Rr* WT CooA at different pH values.

| pH | $K_d$ (nM) |
|---|---|
| 3 | 23±4 |
| 5 | 44±8 |
| 6 | 800±200 |
| 7 | 2500±100 |
| 8 | 15000±2000 |

The major gap in $K_d$ values between pH 5 and 6 is suggestive of a protonation event leading to activity. Upon addition of sodium dithionite to 6 mM and CO to the pH 5 sample, no shift occurred in the anisotropy plot (data not shown). This suggests that the acidic conditions completely convert CooA into the active conformation, leading to maximum activity. However, further studies are required to solidify this claim.

It is also apparent in Figure 5 that DNA binding curves collected at pH 3 and 12 have different baseline anisotropy values in comparison to those curves collected at pH 5-8. The aberrant baseline anisotropy values in base are consistent with pH-dependent interactions of the DNA with the $Ca^{2+}$ ions within solution. At neutral pH, $Ca^{2+}$ interacts strongly with the anionic DNA backbone. As pH increases, $Ca^{2+}$ creates insoluble $Ca(OH)_2$. This causes the DNA to rotate more freely, leading to decreased anisotropy baseline. The aberrant baseline anisotropy values at pH 3 are due to the pH-dependence of the fluorescence life time of Texas Red (Figure 6).[14] Since the fluorescence lifetime of Texas Red increases from 4.15 ns at pH 7 to 4.22 ns at pH 3, this would cause the fluorescence anisotropy to decrease as demonstrated in Equation 2.

Figure 5 also displays DNA binding activity at pH 12. This is observation is consistent with a deprotonation event leading to activity. *Ch* was used to investigate DNA binding affinity at pH 12. This is because *Rr* CooA relies upon $Ca^{2+}$ ions in solution to mediate the interaction between the CooA F-helix and the promoter sequence. Since these ions are insoluble at pH 12, no DNA binding is observed for *Rr*-derived variants.

Interestingly, an induction period of 40 minutes is necessary to observe DNA binding activity at pH 12. This induction period is correlated to the loss of the N-terminal ligand in Figure 6.

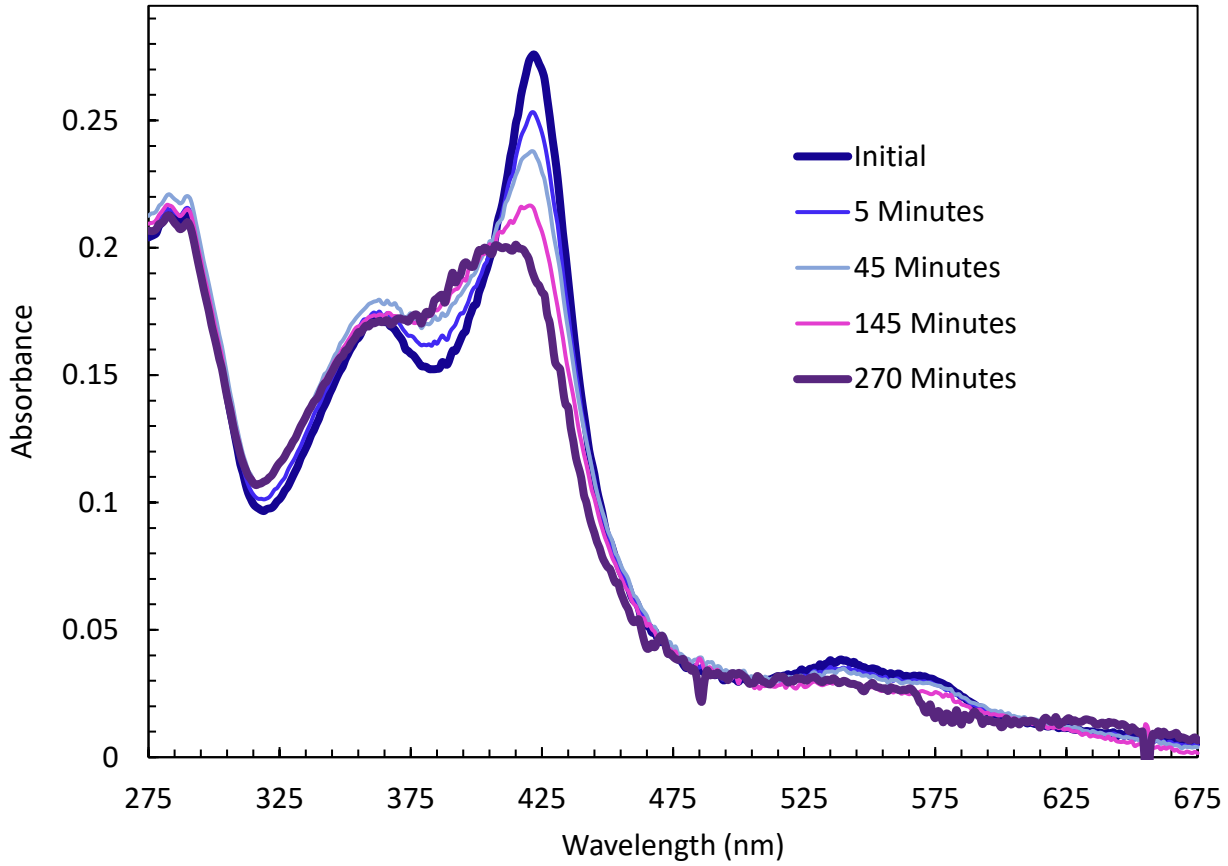


**Figure 6.** UV-Vis spectra of *Rr* CooA at pH 12 (75mM phosphate, 100mM sodium chloride) over time. The loss of the intense peak 424 nm and the growth of the shoulder peak at 385 nm are consistent with the loss of a six-coordinate heme and the generation of a five-coordinate heme, respectively.

The generation of a 5-coordinate heme in basic conditions is consistent with an active CooA conformation, as the N-terminal proline migrates away from the heme iron and towards the DNA-binding domain (see Figure 3). There is no induction period needed to observe DNA binding activity in acidic conditions since the N-terminal proline is likely protonated, further

promoting ligand loss. All CooA variants previously studied at pH 3 by Clark, et al. exhibited 5-coordinate, high spin heme.[4]

To further test the validity of pH dependent CooA-DNA binding, a reversibility study was performed using phosphate buffer, which conveniently has $pK_a$ values near 3, 7 and 12. The results of the anisotropy assays are shown in Figures 7 and 8.

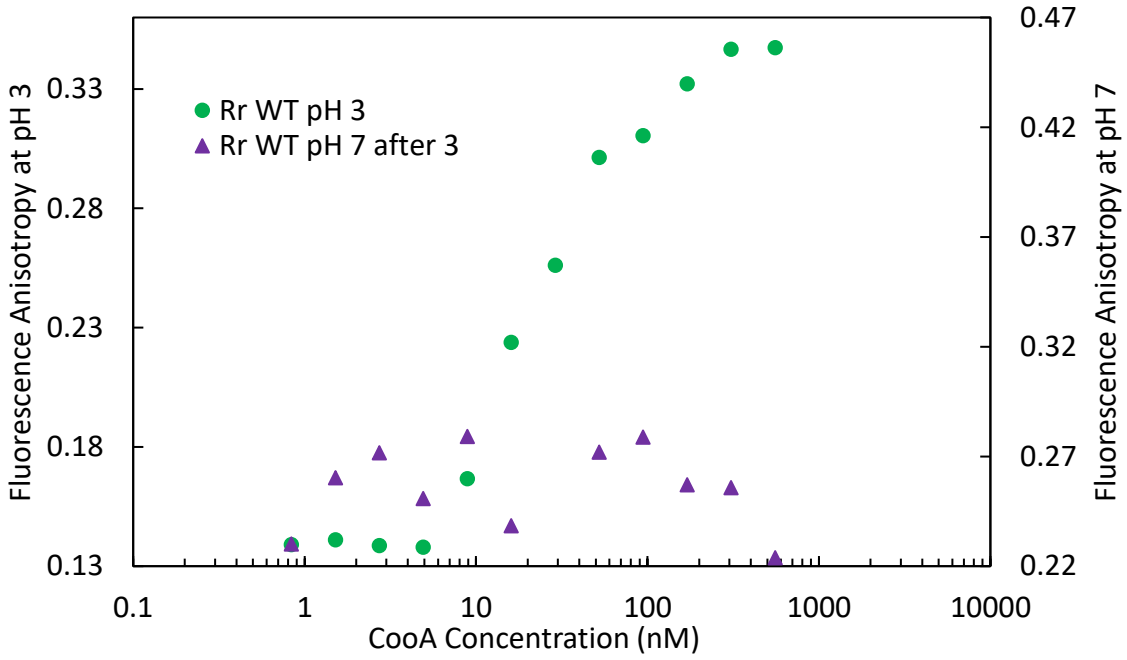


**Figure 7.** Fluorescence anisotropy reversibility experiment of *Rr* CooA at pH 3 then 7. The noisy flat line at pH 7 is interpreted as loss of activity. However, this assay must be recompleted with extra caution paid to the pH of the final solution due to dependence of baseline fluorescence anisotropy on pH.

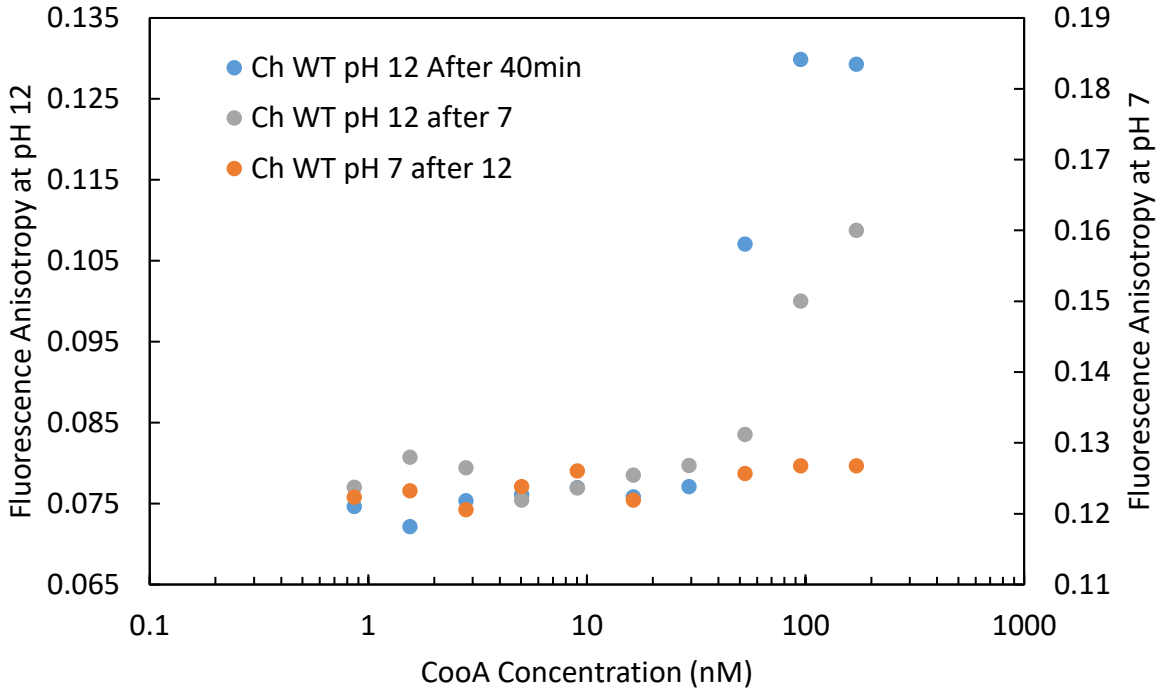


**Figure 8.** Fluorescence anisotropy reversibility experiment of *Ch* CooA samples with Texas Red DNA taken at pH 12 then 7 and 12 to demonstrate reversibility. pH 7 provides a stable flat line, indicating no binding, while binding returns in the pH 12 sample. The secondary pH 12 curve shifts slightly to the right due to moderate protein denaturation over time.

These experiments indicate that the conformation achieved by exposing CooA to acidic and basic conditions is reversible. The protein is not permanently denaturing. However, further tests using circular dichroism spectroscopy are necessary to ensure that the protein is maintaining wild-type secondary structure under the assay conditions.

It is most likely that acidic and basic induced activity occur through a similar mechanism. One such hypothesis for the molecular basis of pH-induced DNA binding revolves around a salt bridge that stabilizes the inactive conformation of CooA. Both acidic and basic conditions would render part of the salt bridge neutral upon protonation or deprotonation, thus breaking the

electrostatic attraction. This action would destabilize the inactive conformation, resulting in an equilibrium shift to the active conformation.

Therefore, if this salt-bridge could be identified, it is possible that a CooA variant in which one of the salt bridge residues is exchanged with a neutral amino acid may exhibit CO-independent activity. After analysis of the inactive and active crystal structures shown in Figures 1 and 3, two evolutionarily conserved salt-bridges were identified that are broken upon activation: E59-R138 (E64-R143 in *Ch* CooA) and D72-R118 (D77-K119). Evolutionary conservation was determined according to an amino acid multiple sequence alignment of known CooA homologs and CRP.[15] It is interesting to note that while D72 is conserved amongst all homologs aligned, R118 is 4 amino acids removed from the conserved location on the C helix. In *Rr*, A114 would be the location of the positive amino acid if it strictly agreed with other CooA homologs. However, this movement should not affect the ability of the amino acid to stabilize the inactive conformation. An analysis of these two salt bridges in the inactive and active CooA crystal structures makes the D72-R118 salt bridge more promising (Figure 9).

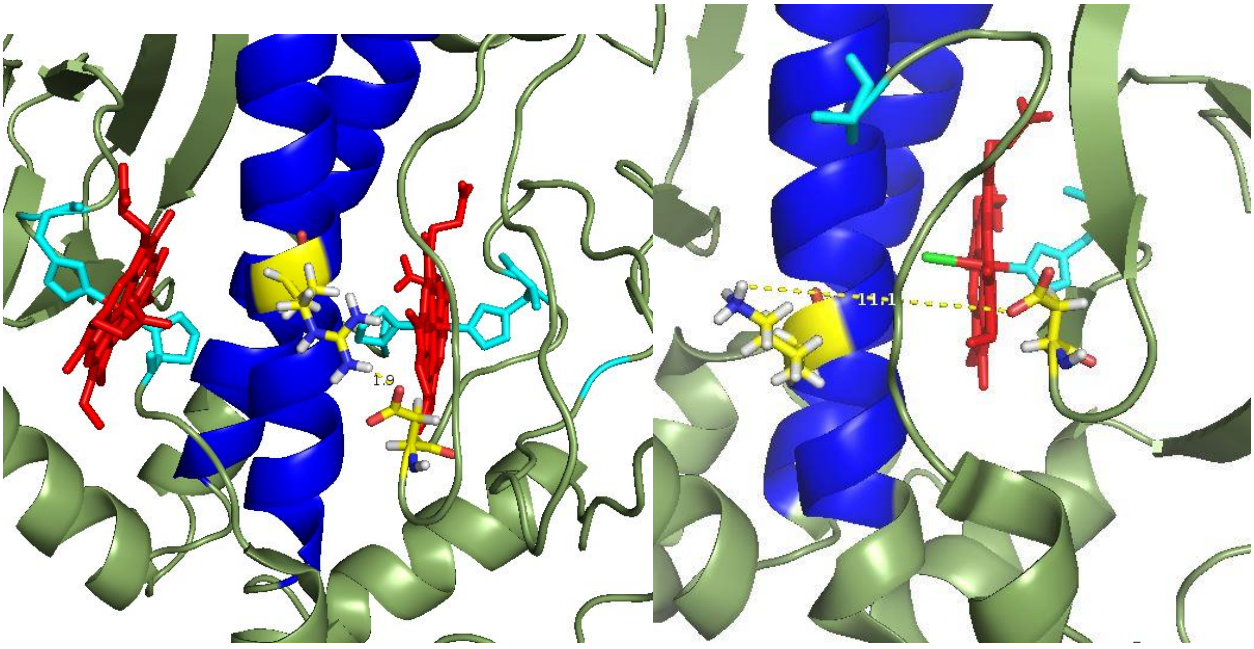

**Figure 9.** Comparison of the D72-R118 salt bridge in inactive (left, PDB: 1FT9) and active (right, PDB: 2HKX) crystal structures. The C helices are shown in blue. D72 and R118 are shown in yellow. The heme is shown in red. Heme ligands are shown in cyan. The two charged residues are 1.9Å apart in the inactive structure and 11.1Å in the active structure.

In the inactive conformation, D72-R118 span the gap between the central C helix and the heme binding pocket. In the active *Ch* structure, K119 seems to have twisted along with the C helix away from D77. Additionally, the N-terminal tail structure of the protein has inserted itself between the two charged residues. Since this change affects the rearrangement of the C helix directly, it seems likely that this salt bridge has an impact on CooA conformational change and DNA binding activity.

To generate a CooA variant with CO independent activity, the following CooA variants were generated via site-directed mutagenesis: D72A, R118D and A114K R118D. These mutations were confirmed by DNA sequencing. At the time of this report, attempts to generate ΔP3R4 analogs of these variants were made; however, DNA sequencing confirmed that the mutations into the ΔP3R4 plasmid were not incorporated.

Fluorescence anisotropy assays of D72A at pH 4 and 7.5 are shown in Figure 10.

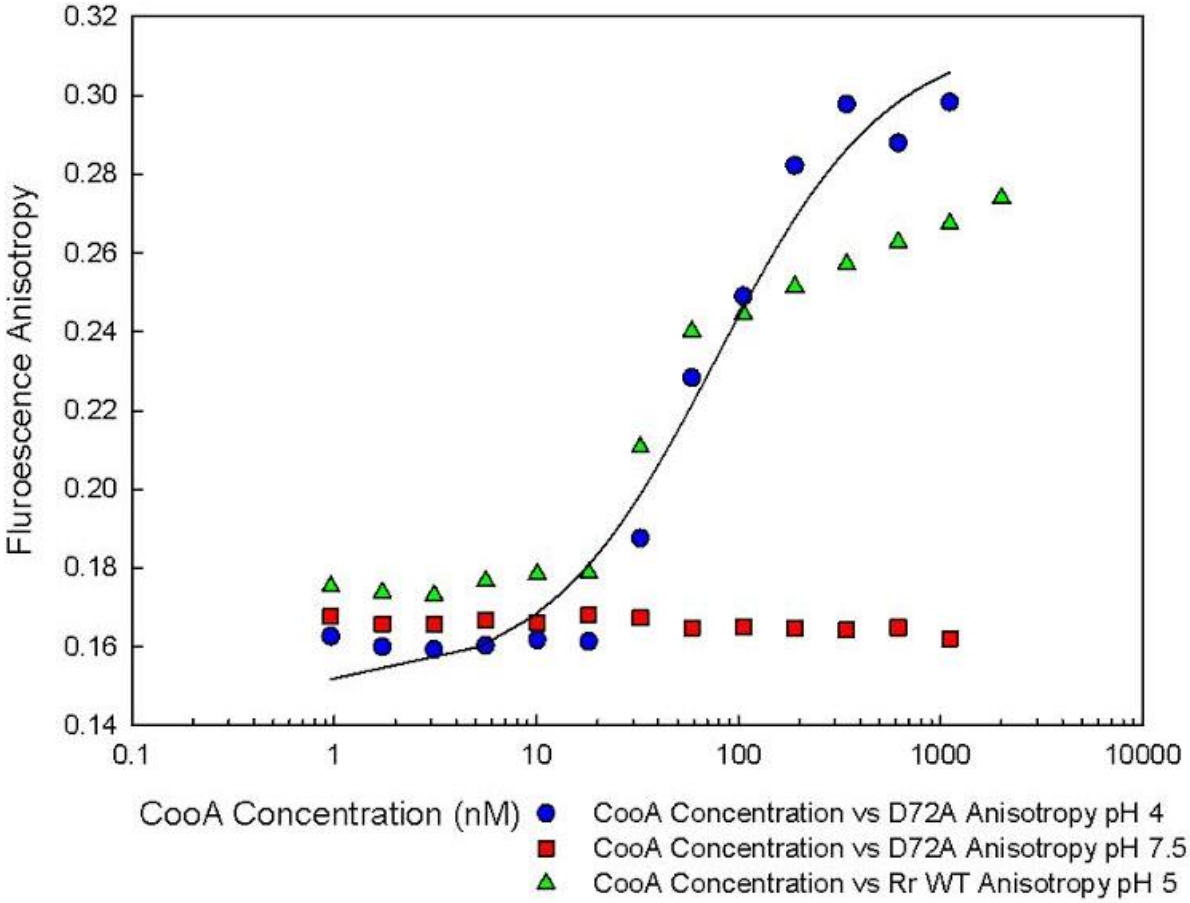


**Figure 10.** Fluorescence anisotropy curves of *Rr.* CooA variant, D72A, at pH 4 and 7.5. The Fluorescence anisotropy curve from *Rr.* Wt at pH 5 is included for comparison. At pH 7.5, no DNA binding is observed, while Wt-like activity of this variant is exhibited at pH 4.

This figure demonstrates that D72A exhibits *Rr* Wt-like DNA binding capabilities at both pH 4 and 7.5. Nonlinear fit of the anisotropy curve at pH 4 provided a $K_d$ value of 74 ± 19 nM. This shows that removing the D72-R118 interaction does not lead to any significant perturbation of DNA binding capabilities at neutral pH. Furthermore, this activity is correlated with D72A exhibiting a 5-coordinate, high-spin heme at pH 3 (Figure 11). This coordination structure is consistent with the active conformation of CooA. This does not deviate from *Rr* Wt-like behavior.

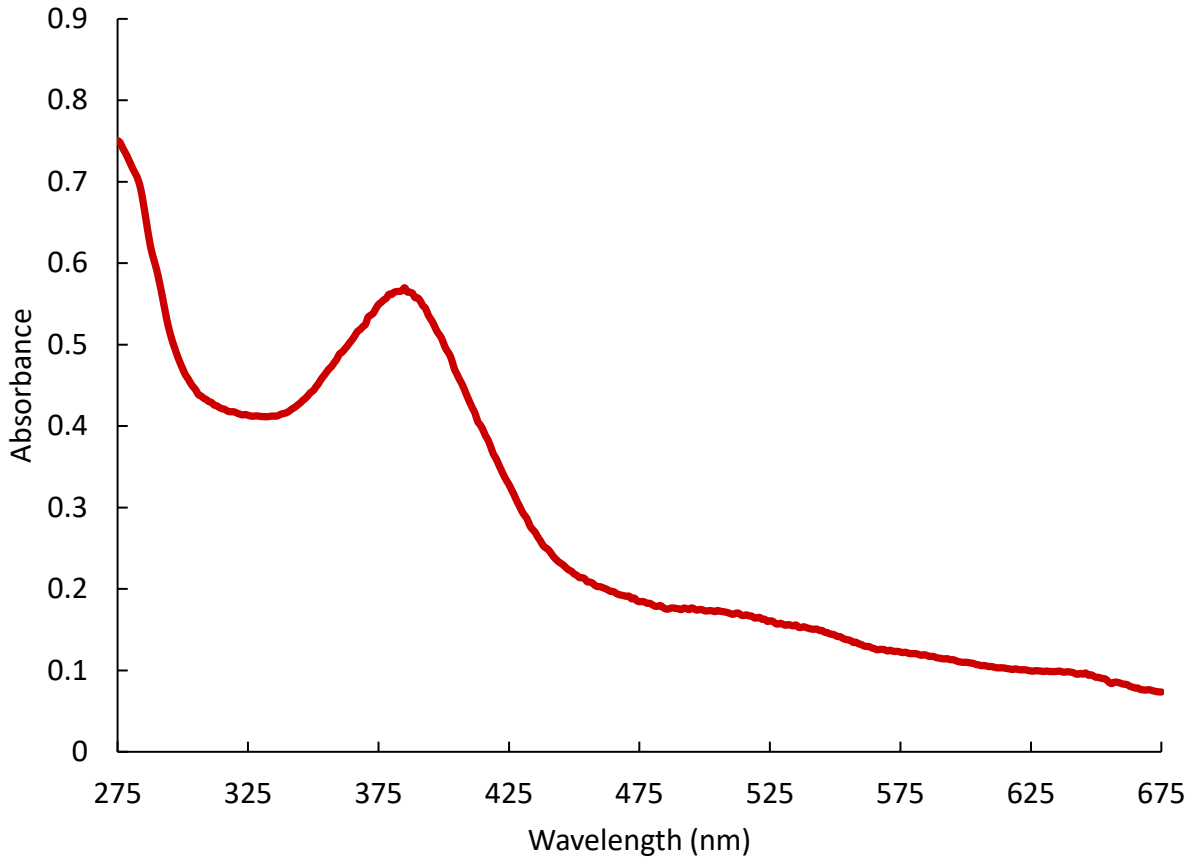


**Figure 11.** Electronic absorption spectrum of D72A CooA at pH 3. 75mM phosphate pH 3 buffer with 100mM sodium chloride was used as a blank. The Soret peak is at 387nm, consistent with a 5-coordinate, high-spin heme.

Fluorescence anisotropy assays quantifying DNA binding affinity of the N-terminal shortening CooA variant, ΔP3R4, have shown activity at pH 4 and no activity at pH 7.5 (data not shown). While the DNA binding capabilities of this variant has been previously characterized at neutral pH[4], acidic activity is a new result for this variant.

Since basic DNA binding assays are not feasible for *Rr* CooA variants, electronic absorption spectroscopy has provided a way to predict DNA binding activity. Experiments looking at coordination structure over time at pH 12 for D72A and ΔP3R4 are shown in Figures 12 and 13, respectively. Figure 12 demonstrates that D72A decays into a 5-coordinate, high-spin heme when placed at pH 12 for long periods of time. This behavior is identical to that of *Rr* Wt.

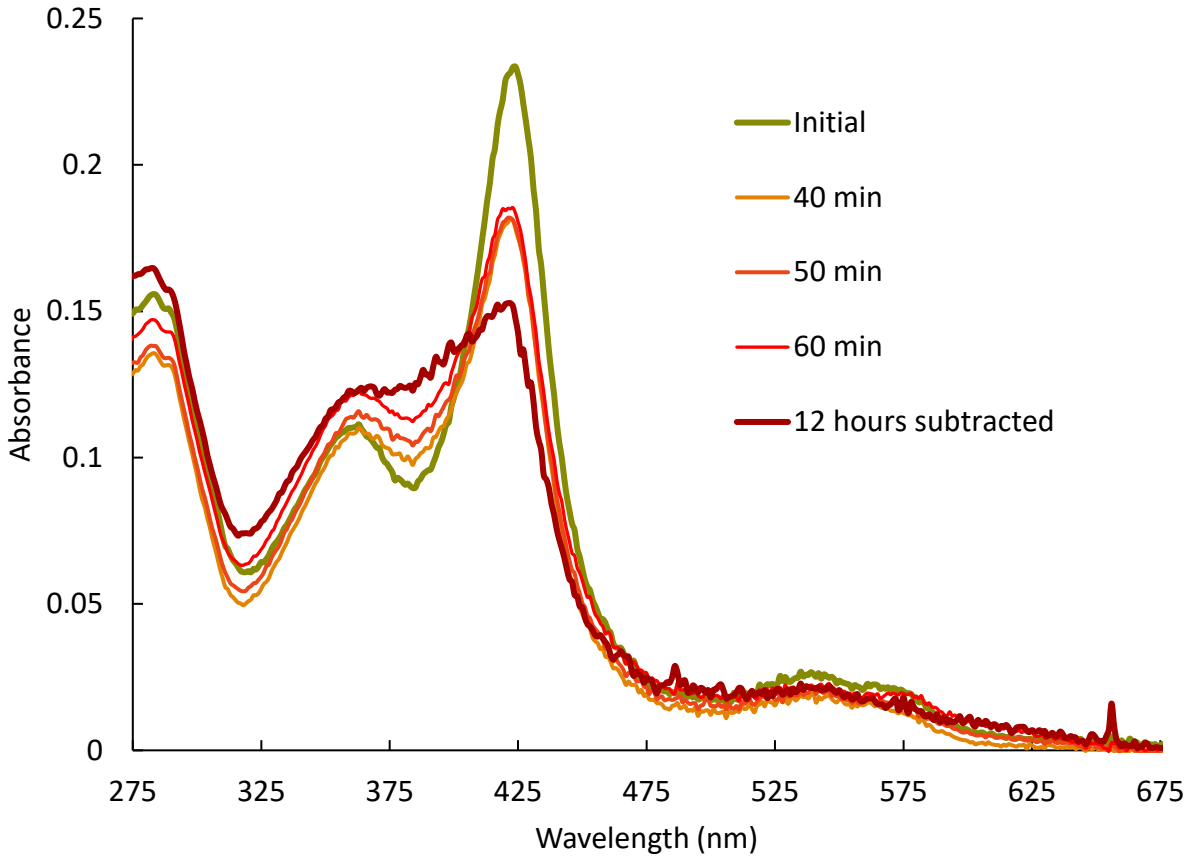


**Figure 12.** Electronic absorbance spectra at pH 12 taken over time for the CooA variant, D72A. This figure demonstrates that this protein decays into a 5-coordinate, high spin heme over time. 75mM phosphate pH 12 buffer with 100mM sodium chloride was used as a blank for these spectra. Since the 12-hour spectrum showed noticeable baseline shift due to protein denaturation, the global minimum, $A_{678}$, was subtracted from the entire spectrum.

Figure 13 demonstrates an unexpected result for ΔP3R4. It has been previously reported that this variant forms a 6-coordinate, low-spin heme in basic conditions.[4] However, since this variant contains a shortened N-terminus that promotes a 5-coordinate, high-spin heme, it was expected that a 6-coordinate structure would decay to a 5-coordinate similar to that of *Rr* Wt. However, spectroscopy shows that this protein forms a stable 6-coordinate, low-spin heme at pH 12. One interpretation could be that the deletion of residues has rendered the N-terminus unable to form

Wt-like contacts at its position in the active conformation pocketed between the DNA-binding and CO-binding domains. This would make the inactive, 6-coordinate conformation of the protein more favorable relative to the active, 5-coordinate conformation.

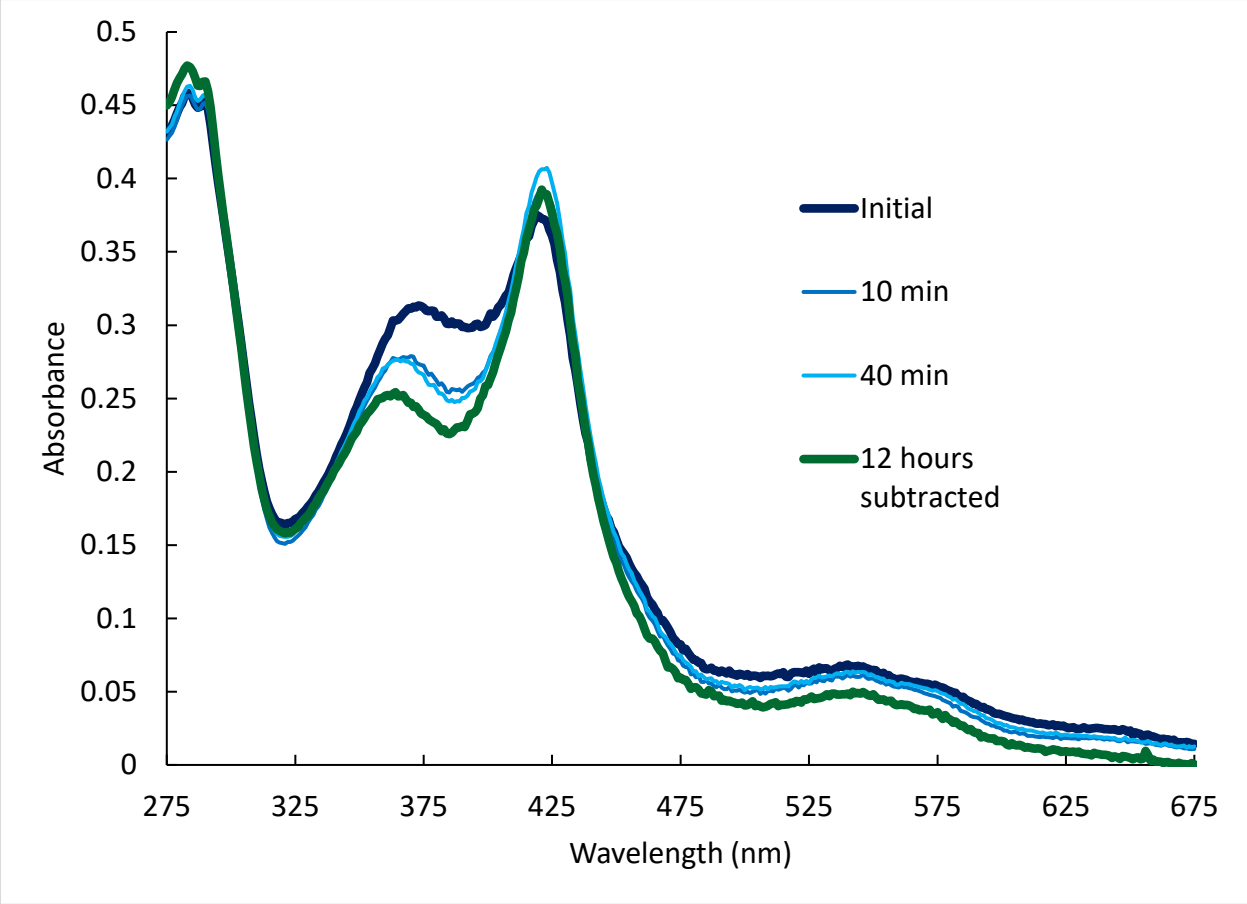


**Figure 13.** Electronic absorbance spectra at pH 12 taken over time for the CooA variant, ΔP3R4. This figure demonstrates that this protein decays from a 5-coordinate, high-spin heme to a 6-coordinate, low-spin heme with time. 75mM phosphate pH 12 buffer with 100mM sodium chloride was used as a blank for these spectra. Since the 12-hour spectrum showed noticeable baseline shift due to protein denaturation, the global minimum, $A_{673}$, was subtracted from the entire spectrum.

Based on these fluorescence anisotropy assays and electronic absorption spectra gathered for D72A and ΔP3R4, it is conclusive that neither removing the D72:R118 salt bridge nor shortening the N-terminus increase CooA DNA binding activity at neutral pH. However, the lack

of activity in each of these mutants could be the result of the salt-bridge and N-terminal ligation acting as stabilizing forces. In other words, both the N-terminus must be displaced as well as the salt bridge must be removed for activity to be observed. This lends itself to a "double roadblock" model of understanding pH-induced DNA binding activity, where loss of the N-terminus and the salt bridge are independent stabilizing forces that must be overcome to observe CooA activity at neutral pH. Based on this model, the CooA mutant, ΔP3R4 D72A, should demonstrate intrinsic DNA binding activity.

**Conclusions:**

pH-induced DNA binding activity has been characterized and quantified in both acidic and basic conditions, demonstrating that CooA can be led to bind DNA in the Fe(III) state with Wt-like affinity. The robustness of this sort of DNA binding activity was highlighted in fluorescence anisotropy assays which alternate between neutral, acidic and basic pH values. Activity is also correlated with the generation of 5-coordinate heme structures, consistent with the active conformation of CooA. Using insight from amino acid conservation among CooA homologs, the D72:R118 salt bridge was identified as a potential source of this aberrant activity. However, neither the N-terminal shortening variant, ΔP3R4, nor D72A provided activity at neutral pH.

This work highlights the need to revise current models of CooA conformational change. The current model states that CO binding to the heme iron and displacing the N-terminus causes the heme pocket to rearrange. This rearrangement causes the central helices to twist, which leads to rearrangement of the DNA binding domain, exposing the F helices that bind the major grooves of the promoter sequence. The pH-induced DNA binding reported here highlights the role of salt

bridges in stabilizing the inactive conformation. Subsequent CooA activation models must account for breaking these interactions as part of conformational change.

**Future Work:**

Future work on this project begins with expressing and purifying the CooA variants R118D and A114K R118D. Additionally, quantification of DNA-binding activities will be completed for all CooA variants at pH 3, 4, 5, 6, 7, and 8 using the fluorescence anisotropy assay.

Due to protonation under acidic conditions, CooA molecules will have a net positive charge. Since DNA is natively anionic, these two molecules would naturally associate in solution. However, this association would be non-specific for the DNA sequence unlike typical CooA-DNA binding in which the $P_{coof}$ sequence is bound preferentially. To control for anisotropic increases due to non-specific binding, unlabeled, non-$P_{coof}$ DNA will be added to all future fluorescence anisotropy assays.

Since basic DNA binding activities cannot be quantified for *Rr*-derived CooA variants, *Ch* CooA variants analogous to D72A, R118D and A114K R118D will be generated via site-directed mutagenesis. These variants will then be used to quantify basic DNA binding activity since *Ch* CooA has no dependence on calcium ions to bind DNA.

To clear uncertainties regarding protein conformation in acidic and basic conditions, circular dichroism spectroscopy will be completed. This spectroscopy is used to probe the secondary structure present in proteins. Specifically, spectra will be gathered for *Rr* and *Ch* Wt at pH 3, 4, 5, 6, 7 and 8. Upon comparison of these spectra, if no major changes in absorbance is observed, this would suggest that CooA secondary structure is stable and not denatured under these assay conditions and CooA is in its active conformation.

**References:**


[1] Roberts, G. P.; Youn, H.; Kerby, R. L. CO Sensing Mechanisms. *Microbiol Mol Biol Rev* **2004**, *68*(3), 453–473.

[2] Lanzilotta,W.; Schuler, D. J.; Thorsteinsson, M. V.; Kerby, R. L.; Roberts, G. P.; Poulos, T. L. Structure of the CO sensing transcription activator CooA. *Nat. Struct. Biol.* **2000**, *7*(10) 876-883.

[3] Clark, R. W.; Youn, H.; Lee, A. J.; Roberts, G. P.; Burstyn, J. N. DNA binding by an imidazole-sensing CooA variant is dependent on the heme redox state. *J. Biol. Inorg. Chem.*, **2007**, *12*(2), 139-146.

[4] Clark, R. W.; Youn, H.; Parks, R. B.; Cherney, M. M.; Roberts, G. P.; Burstyn, J. N. Investigation of the role of the N-terminal proline, the distal heme ligand in the CO sensor CooA *Biochemistry* **2004**, *43*(44), 14149–14160.

[5] Komori, H.; Inagaki, S; Yoshioka, S.; Aono, S.; Higuchi, Y. Crystallization and preliminary X-ray analysis of CooA from *Carboxydothermos hydrogenoformans*. *Acta Cryst.* **2006**, *F62*, 471-473

[6] Ibrahim, M.; Kerby, R. L.; Puranik, M.; Wasbotten, I. H.; Youn, H.; Roberts, G. P.; Spiro, T. G. Heme Displacement Mechanism of CooA Activation: Mutational and Raman Spectroscopic Evidence. *J. Biol. Chem.* **2006**, *281*(39), 29165-29173.

[7] Borjigin, M.; Li, H.; Lanz, N. D.; Kerby, R. L.; Roberts, G. P.; Poulos, T. L. Structure based hypothesis on the activation of the CO-sensing transcription factor CooA. *Acta Cryst.* **2007**, *D63*, 282-287.

[8] Schultz, S.C.; Shields, G.C.; Steitz, T.A. Crystal structure of a CAP-DNA complex: the DNA is bent by 90 degrees. *Science*, **1991**, *253*, 1001-1007.

[9] Thorsteinsson, M. V.; Kerby, R. L.; Conrad, M.; Youn, H.; Staples, C. R.; Lanzilotta, W. N.; Poulos, T. J.; Serate, J.; Roberts, G. P. Characterization of Variants Altered at the N-terminal Proline, a Novel Heme-Axial Ligand in CooA, the CO-sensing Transcriptional Activator. *J. Biol. Chem.* **2000**, *275*, 39332-39338.

[10] Lundblad, J. R.; Laurence, M.; Goodman, R. H. Fluorescence Polarization Analysis of Protein-DNA and Protein-Protein Interactions. *Molecular Endocrinology*, **1996**, *10*(6), 607-612.

[11]Stewart, V.; Lu, Y.; Darwin, A. J. Periplasmic Nitrate Reductase (NapABC Enzyme) Supports Anaerobic Respiration by *Escherichia coli*. *J. Bact.* **2002**, *184*, 1314-1323..

[12]Shelver, D.; Kerby, R. L.; He, Y.; Roberts, G. P. CooA, a CO-sensing transcription factor from *Rhodospirillum rubrum*, is a CO-binding heme protein. **1997**, *94*(21), 11216-11220..

[13] Inagaki, S.; Masuda, C.; Akaishi, T.; Nakajima, H.; Yoshioka, S.; Ohta, T.; Pal, B.; Kitagawa, T.; Aono, S. Spectroscopic and Redox Properties of a CooA Homologue from *Carboxydothermus* h*ydrogenoforman*. **2005**, *280*(5), 3269-3274.

[14] Brismar, H.; Trepte, O.; Ulfhake, B. Spectra and Fluorescence Lifetimes of Lissamine Rhodamine, Tetramethylrhodamine Isothiocyanate, Texas Red, and Cyanine 3.18 Fluorophores: Influences of Some Environmental factors Recorded with a Confocal Laser Scanning Microscope. *Journal of Histochemistry and Cytochemistry*, **1995**, *43*(7) 699-707.

[15] Youn, H.; Kerby, R. L.; Conrad, M.; Roberts, G. P. Functionally Critical Elements of CooA-Related CO Sensors. *J. Bacteriol*., **2004**, *186*(5), 1320-1329.